



**Cascaded optical limiter with low activating and high damage thresholds using single-layer graphene and single-walled carbon nanotubes**

Yaobing Xiong, Lihe Yan, Jinhai Si, Wenhui Yi, Wen Ding, Wenjiang Tan, Xin Liu, Feng Chen, and Xun Hou

Citation: [Journal of Applied Physics](#) **115**, 083111 (2014); doi: 10.1063/1.4867155

View online: <http://dx.doi.org/10.1063/1.4867155>

View Table of Contents: <http://scitation.aip.org/content/aip/journal/jap/115/8?ver=pdfcov>

Published by the [AIP Publishing](#)

---



## Re-register for Table of Content Alerts

Create a profile.



Sign up today!



# Cascaded optical limiter with low activating and high damage thresholds using single-layer graphene and single-walled carbon nanotubes

Yaobing Xiong,<sup>1</sup> Lihe Yan,<sup>1</sup> Jinhai Si,<sup>1,a)</sup> Wenhui Yi,<sup>1</sup> Wen Ding,<sup>1</sup> Wenjiang Tan,<sup>1</sup> Xin Liu,<sup>2</sup> Feng Chen,<sup>1</sup> and Xun Hou<sup>1</sup>

<sup>1</sup>*School of Electronic & Information Engineering, Xi'an Jiaotong University, Xi'an 710049, People's Republic of China*

<sup>2</sup>*Science and Technology on Electro-Optical Information Security Control Laboratory, Sanhe 065201, People's Republic of China*

(Received 22 December 2013; accepted 17 February 2014; published online 27 February 2014)

The optical limiting (OL) properties of single-layer graphene dispersions at 532 and 1064 nm wavelengths were investigated using a nanosecond laser. The experimental results show that the activating threshold of the single-layer graphene dispersed in chlorobenzene (CB) is lower than that of single-walled carbon nanotubes (SWNTs) by a factor of 10. The nonlinear scattering experiments for the graphene dispersions indicate that the main mechanism of the OL properties is nonlinear scattering effect, whereas nonlinear absorption might contribute to the OL effect of graphene in CB. To enlarge the damage threshold of the limiter, we propose a cascaded optical limiter by combining the advantages of low activating threshold for the graphene and the high damage threshold for the SWNTs. The cascaded optical limiter shows a low activating threshold, a high damage threshold, and broadband OL properties. © 2014 AIP Publishing LLC. [<http://dx.doi.org/10.1063/1.4867155>]

## I. INTRODUCTION

Optical limiting (OL) is a very important nonlinear optical phenomenon in protecting optical sensors and the human eyes.<sup>1–7</sup> In general, a good OL material must have the following characteristics. First, its activating threshold should be as low as possible for protecting various delicate optical devices and the eyes. Second, it must respond instantaneously to any laser pulse with durations ranging from a few picoseconds to continuous wave. Finally, it must operate over a wide wavelength range from visible to infrared region.

Much effort has been devoted to the development of optical limiters with larger nonlinear responses from carbon-based materials.<sup>8,9</sup> The OL properties of single-walled carbon nanotubes (SWNTs) have been investigated extensively for over a decade.<sup>2,4,10</sup> The experimental results indicate that the optical limiters using SWNTs show a high damage threshold and suitable for a wide wavelength range from the visible to the infrared regions. This is because of the nonlinear scattering mechanism of the OL resulting from the formation of solvent microbubbles and carbon microplasma.<sup>4,11–13</sup>

With the emergence of graphene, the excellent electronic, thermal conductivity, and optical properties of graphene have attracted significant research interest.<sup>14–19</sup> Meanwhile, investigations of the nonlinear optical properties of graphene made a significant progress.<sup>20–22</sup> For example, Hendry *et al.* studied the coherent nonlinear optical response of graphene, which showed a remarkably large third-order susceptibility.<sup>20</sup> Nesterov *et al.* studied nonlinear propagation of light in a graphene monolayer, demonstrating the formation of subwavelength spatial solitons.<sup>21</sup> Since the first report by Wang *et al.*,<sup>23</sup> much efforts have been devoted to study the OL properties of

graphene, graphene oxide, and their composites with various molecules.<sup>24–29</sup> For example, Lim and co-workers investigated the nonlinear response of single-layer graphene oxide in appropriate solvents or film matrices and demonstrated excellent OL properties based on broadband nonlinear absorption effect.<sup>24</sup> Chantharasupawong *et al.*<sup>28</sup> reported the excellent OL property of fluorinated graphene oxide. Generally, graphene materials have been demonstrated to possess an outstanding OL ability as well as good dispersity in various solvents, making them potential candidates for optical limiters.

In this study, we investigate the OL behavior of single-layer graphene dispersions in different solvents. The single-layer graphene dispersed in chlorobenzene (CB) shows very low activating threshold for nanosecond laser pulses at both 532 and 1064 nm wavelengths. The pulse energy dependence of the scattered light intensity indicated that the OL behavior of the graphene dispersions is mainly originated from the nonlinear scattering effect, whereas nonlinear absorption might contribute to the OL effect of graphene in CB. Despite of its ultralow OL threshold, the graphene dispersion is easily destroyed when the laser pulse density exceed a damage threshold. To enlarge the dynamic range of the input energy density, we propose a cascaded optical limiter composed by two adjacent sample cuvettes filled with SWNTs dispersion and graphene dispersion, respectively. By combining the advantages of low activating threshold of the graphene dispersion and high damage threshold of SWNTs dispersion, the cascaded optical limiter shows the characteristics of low activating threshold, high damage threshold, as well as broadband OL properties.

## II. EXPERIMENTAL DETAILS

The SWNTs (length: 5–30  $\mu\text{m}$ , diameter: 0.8–1.6 nm, purity: >90%) were obtained from Chengdu Organic Chemicals

<sup>a)</sup>E-mail: jinhaisi@mail.xjtu.edu.cn.

Co., Ltd., (Chengdu, china). The single-layer graphene (thickness:  $\sim 0.8$  nm, diameter:  $0.5\text{--}2$   $\mu\text{m}$ , purity:  $\sim 99\%$ , single layer ratio:  $>80\%$ ) was obtained from Nanjing XFNano Materials Tech Co., Ltd., (Nanjing, China). The SWNTs and single-layer graphene were dispersed in N-methyl-2-pyrrolidinone (NMP) and CB, respectively. The four dispersions were prepared by adding 6 mg of materials in 40 ml of solvents, and then sonicated for 2 h in an ice bath. All dispersions were subsequently centrifuged at 5000 rpm for 30 min to remove any large aggregates. The samples were stable against sedimentation and with litter aggregation occurring in a few days. The morphology of the dispersed graphene was observed using transmission electron microscopy (TEM, JEOL JEM-2100). The TEM samples were prepared by dropping a few milliliters of each dispersion on copper holey carbon grids. Figures 1(a) and 1(b) show the typical TEM image of graphene dispersed in CB and NMP, respectively. The graphene samples were mainly stretched on copper grids in single-layer form with a little scrolled edges or folded region. Large flakes with multilayer were seldom observed by TEM in our dispersions, indicating that a high percentage of our samples in solvents was single-layer graphene.

In this study, all the experiments were performed using a 10 ns pulse from a Q-switched  $\text{Nd}^{3+}$ : YAG laser. The laser source was spatially filtered to remove the higher-order modes and obtain a neat Gaussian beam profile, and then tightly focused with a lens of 35 cm focal length. The laser was operated at the fundamental wavelength of 1064 nm, and the second harmonic of 532 nm, with a pulse repetition rate of 10 Hz. An open-aperture Z-scan system is used to study the OL behavior of the dispersions. All the dispersions were filled in a 5 mm thick quartz cells, and the linear transmittances of the samples could be adjusted by changing the concentrations.

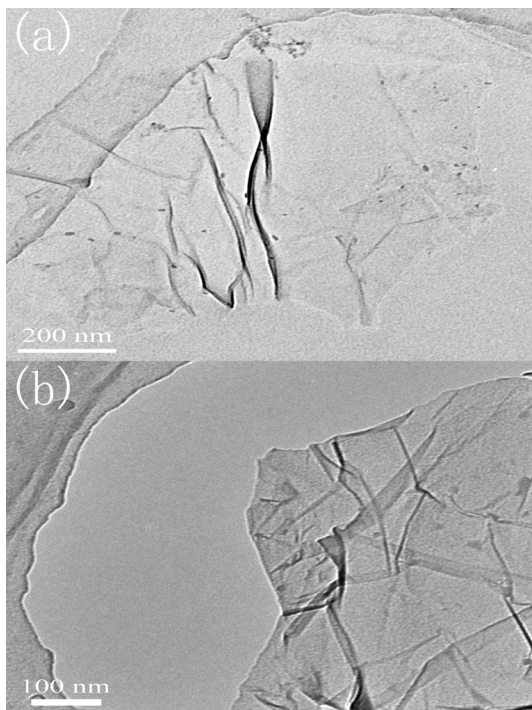


FIG. 1. (a) TEM image of single-layer graphene dispersed in (a) CB and (b) NMP.

### III. RESULTS AND DISCUSSION

#### A. OL behaviors and mechanisms of single-layer graphene dispersions

First, we measured the OL properties of four dispersions, SWNTs in N-methyl-2-pyrrolidinone (SWNTs-NMP), SWNTs dispersed in chlorobenzene (SWNTs-CB), single-layer graphene dispersed in NMP (G-NMP), and single-layer graphene dispersed in chlorobenzene (G-CB), respectively. Figures 2(a) and 2(b) show the variation in output fluence as a function of the input fluence at 532 nm and 1064 nm, respectively. The red, green, blue, and purple scatters in the figures indicate the OL performance of SWNTs-NMP, SWNTs-CB, G-NMP, and G-CB dispersions, respectively. All of them were calculated from the Z-scan data.<sup>28</sup> The linear transmittance was adjusted to 70%. It is evident from Fig. 2 that SWNTs-NMP afforded similar OL characteristics as SWNTs-CB and G-NMP dispersions, while G-CB dispersion showed much more excellent OL ability than those three former samples. There was not any variation of the transmittance of the NMP or CB solvent observed at the same input energy density. Hence, the contribution of the solvent itself to the OL behavior was ruled out. The OL threshold of G-CB dispersion is estimated to be  $0.08 \text{ J cm}^{-2}$  (where transmittance falls to 50% of linear transmittance), which was similar as that of the graphene dispersions has been reported by Lim *et al.* (using a laser with a pulse width of 3.5 ns),<sup>24</sup>

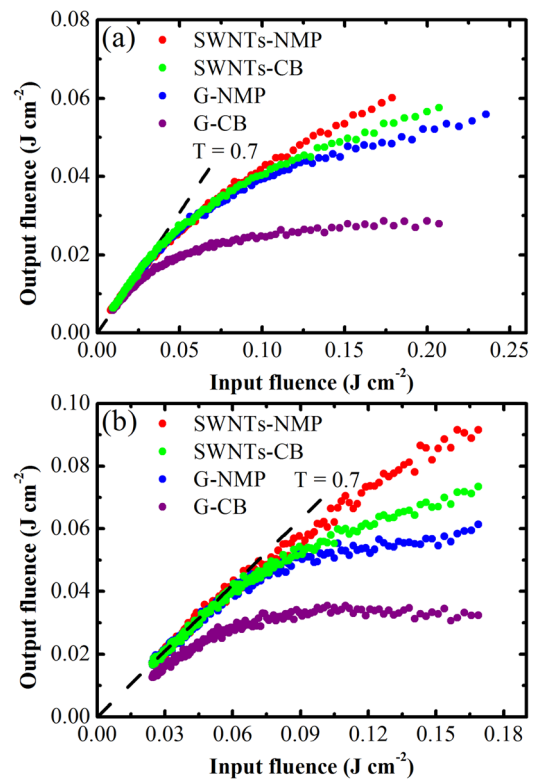


FIG. 2. Linear and nonlinear transmittance characteristics of SWNTs and graphene dispersions: (a) plot of the output fluence vs. input fluence for SWNTs and graphene dispersions at 532 nm and (b) variation in the output fluence as a function of the input fluence at 1064 nm.  $T$  is the linear transmittance fixed at 70%. All of them were calculated from the Z-scan data for different samples.

being about 5–10 times lower than those in the previous reports.<sup>28,29</sup>

It is well known that OL behavior of carbon materials arises mainly from nonlinear absorption and/or nonlinear scattering. In the previous reports, people have demonstrated the different mechanisms of graphene materials in various surrounding environments.<sup>23,24</sup> For example, Lim *et al.* demonstrated the giant broadband nonlinear optical absorption response in dispersed graphene single sheets using a nano-second pump–probe spectroscopy,<sup>24</sup> whereas Wang claimed that the OL behavior of graphene was mainly attributed to the nonlinear scattering effect.<sup>23</sup> To elucidate the mechanisms of the OL effect of the graphene dispersions in our experiments, the pulse energy dependence of the scattered light intensity was measured by collecting a fraction of the scattered light using a convex lens at  $\sim 30^\circ$  in the forward direction from the beam axis. For the measurements, the energy of the scattered light passing through a suitably positioned 4 mm diameter aperture was collected using a photodiode. Figure 3 shows the variations of the nonlinear transmittances and scattering intensities of the dispersions as functions of the input pulse energy density. As shown by the figure, the scattered signal increased significantly with the decrease in the transmission, and the onset of the growth of the scattered signals was synchronous with the onset of the decrease of the transmission for all the dispersions, indicating that nonlinear scattering was the main mechanism responsible for the observed OL properties.

In the OL process, graphene or SWNTs in dispersions were heated by the intense light and transferred the thermal energy to the surrounding solvents. When the temperature was high enough, the surrounding solvents would be evaporated, resulting in the formation of gas bubbles. The initial bubbles quickly expanded to the magnitude of incident light wavelength and induced the scattering of the incident light, causing the reduction of transmittance. In the equilibrium condition, the bubble size could be defined by the following equations:<sup>7,30</sup>

$$2\gamma = \frac{3nRT}{4\pi r_B^2} - p_\infty r_B, \quad (1)$$

where  $\gamma$  is the surface tension,  $n$  is the number of moles of gas,  $R$  is the universal gas constant,  $T$  is the absolute

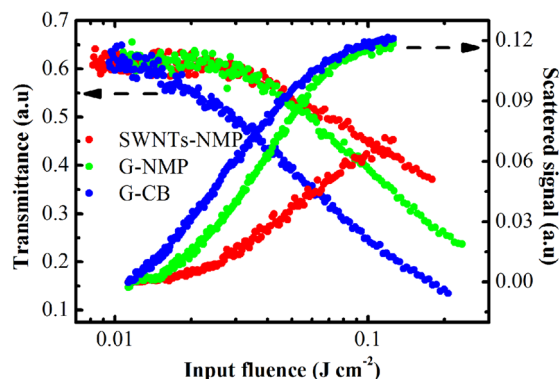


FIG. 3. Transmission and scattered signals as functions of the incident pulse energy density for three dispersions at 532 nm. The linear transmittance is 60%.

temperature in the bubble.  $r_B$  is the bubble size, and  $P_\infty$  is the pressure far from the bubble. From Eq. (1), a lower surface tension results in a larger bubble size, hence, producing more effective scattering and promoting OL behavior. Therefore, the lower activating threshold of the G-CB dispersion in our experiments could be mainly attributed to the lower surface tension of the CB solvent than that of NMP.

It should be noticed that when the input fluence is higher than  $0.1 \text{ J cm}^{-2}$ , in our experiments, the transmittance of G-CB is much lower than G-NMP, while the scattered signal intensity of G-CB and G-NMP is almost equal (as shown in Fig. 3). It indicates that the mechanism of the OL of the G-CB does not only come from nonlinear scattering, but also might be due to nonlinear absorption. As claimed by Lim, nonlinear optical absorption might occur when the single-layer graphene was dispersed in heavy atom solvents, such as CB.<sup>24</sup> Hence, we measured the OL behavior of single-layer graphene films on a quartz plate. The graphene film was first grown on a nickel layer and then transferred to the quartz plate. To investigate the solvent effect on the nonlinear absorption, the quartz plate with graphene film was emerged in a cell filled with CB and NMP, respectively. As the graphene material was adhered on plate, no scattering center was able to be formed in the solvent, and the contribution of nonlinear scattering effect was excluded. The results showed the transmittance of the single-layer graphene film in CB decreased with increasing the input pulse energy, while those of the CB solvent without graphene film and NMP with graphene film kept the same as the linear transmittance, indicating that nonlinear absorption effect occurred in the single-layer graphene film in CB. In conclusion, the OL effect of the graphene dispersions is mainly originated from the nonlinear scattering effect, whereas nonlinear absorption might also contribute in CB solvent due to the heavy atom effect.

## B. Cascaded optical limiter based on single-layer graphene dispersions

Single-layer graphene dispersion in CB exhibited excellent OL properties, however, the graphene flakes were easily aggregated after successive irradiation by the laser pulses when the input fluence exceeded  $0.25 \text{ J cm}^{-2}$ . The low damage threshold will limit the applications of the limiter to a very small input fluence range. In the practical applications, an excellent optical limiter does not only need to have an ultra-low activating threshold, but also is expected to be able to work well in a broad dynamic range of the input energy.

Based on this consideration, we propose a cascaded optical limiter based on single-layer graphene dispersions. The laser beam was first irradiated into the cuvette filled with SWNTs-NMP dispersion and then irradiated the adjacent cuvette filled with G-CB dispersion. The SWNTs-NMP dispersion was used as the first protection layer, and the G-CB dispersion as the second protection layer. As SWNTs-NMP exhibited a high damage threshold and a broadband OL property in our experiments, an intense laser pulse will be attenuated first by the SWNTs-NMP dispersions when it irradiated into the cascaded limiter, ensuring the output intensity of the first protection layer being below the damage

threshold of G-CB. When the laser beam passed the second protection layer, G-CB dispersion would limit the transmission of the incident light greatly due to its much lower OL activating threshold. The cascaded optical limiter combines the advantages of low activating threshold of G-CB and high damage threshold of SWNTs-NMP.

Figure 4(a) shows the output fluence vs. the input fluence at 532 nm. The linear transmittances of SWNTs-NMP and G-CB dispersions were 60%, and that of the cascaded optical limiter (SWNTs-NMP/G-CB) was 36%. From the figure, we can see that the G-CB dispersion shows a small dynamic range as shown by the blue squares. When the input fluence was above  $0.25 \text{ J cm}^{-2}$ , the dispersion would form aggregation, i.e., the sample was damaged. In contrast, SWNTs-NMP dispersion showed a much higher damage threshold up to  $1.4 \text{ J cm}^{-2}$ , as shown by the red squares. Because the output influence of SWNTs-NMP was about  $0.25 \text{ J cm}^{-2}$ , it could protect the second layer filled with G-CB from damage in the cascaded limiter. The violet scatters in Fig. 4(a) indicate the OL behaviour of the cascaded optical limiter. The maximum incident light intensity can reach to higher than  $1.3 \text{ J cm}^{-2}$ , and the maximum output intensity keeps below  $0.05 \text{ J cm}^{-2}$ . Figure 4(b) shows the amplification of the rectangle in Fig. 4(a). As indicated by the dashed red line, when the input fluence was  $0.25 \text{ J cm}^{-2}$ , the output fluence was about  $0.09 \text{ J cm}^{-2}$  for the SWNTs-NMP dispersion. As indicated by the dashed violet line, when the G-CB dispersion was cascaded with the first protection layer, the output fluence was decreased to be about  $0.03 \text{ J cm}^{-2}$ , which was in accordance

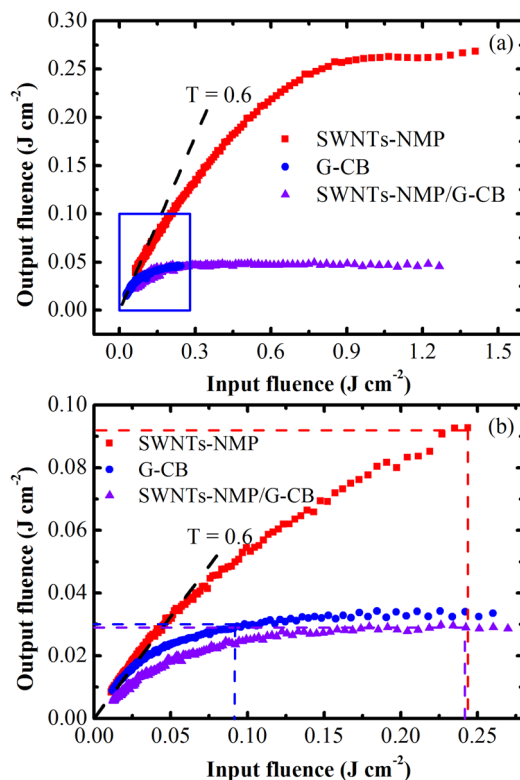


FIG. 4. The characteristics of cascaded optical limiter: (a) variation in the output fluence as a function of the input fluence at 532 nm and (b) the amplification plot of the rectangle in Fig. 4(a). The linear transmittance is adjusted to 60% at 532 nm.

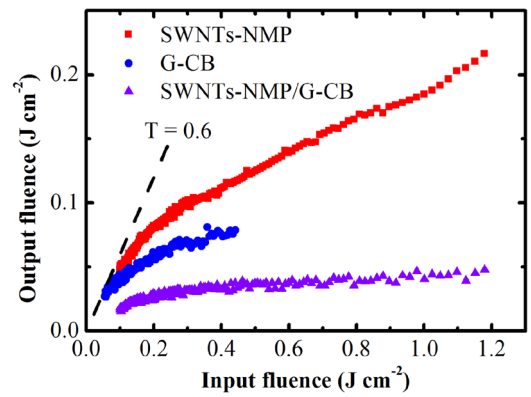


FIG. 5. OL behaviour of SWNTs-NMP, G-CB, and SWNTs-NMP/G-CB dispersions at 1064 nm. The linear transmittance is 60% for SWNTs-NMP and G-CB samples, whereas it is about 36% for the cascaded optical limiter.

with the output of the single G-CB dispersion at an input fluence of  $0.09 \text{ J cm}^{-2}$  (pointed out by the blue line). Therefore, we can conclude that the cascaded optical limiter not only maintained the low limiting activating threshold of the G-CB dispersion, but also inherited the high damage threshold of the SWNTs-NMP dispersion. The damage threshold of the cascaded optical limiter was about 5 times larger than G-CB dispersion, while the OL threshold kept the same with that of G-CB dispersion, being about more than 5 times lower than those in the previous reports.<sup>28,29</sup>

Figure 5 shows the output fluence of the cascaded optical limiter vs. the input fluence at 1064 nm similar to the OL behaviour at 532 nm. The cascaded optical limiter showed a much higher damage threshold than G-CB dispersion and a much lower activating threshold than SWNTs-NMP dispersion. The maximum incident light intensity can reach to  $1.2 \text{ J cm}^{-2}$ , and the maximum output intensity kept below  $0.05 \text{ J cm}^{-2}$ . Hence, the cascaded optical limiter showed not only a high damage threshold, an ultra-low activating threshold, but also a broadband OL ability from the visible to the infrared regions.

#### IV. CONCLUSIONS

In summary, we experimentally studied the efficient OL behaviour of three different dispersions using 532 and 1064 nm nanosecond laser pulses. The results clearly demonstrate that the activating threshold of the G-CB dispersion exceeded that of SWNTs-NMP dispersion by a factor of 10. The measurements reveal that the main mechanism of the OL was nonlinear scattering. By integrating the advantages of G-CB and SWNTs-NMP dispersions, i.e., the low activating threshold for G-CB and the high damage threshold for SWNTs-NMP, we proposed and designed a cascaded optical limiter. The cascaded optical limiter exhibited low activating threshold, high damage threshold, and broadband OL characteristics.

#### ACKNOWLEDGMENTS

The authors gratefully acknowledge the support from the National Science Foundation of China (Grant No. 61235003) and the National Basic Research Program of China (973 Program) (Grant No. 2012CB921804).

- <sup>1</sup>L. Vivien, D. Riehl, P. Lancon, F. Hache, and E. Anglaret, *Opt. Lett.* **26**, 223 (2001).
- <sup>2</sup>L. Vivien, P. Lancon, D. Riehl, F. Hache, and E. Anglaret, *Carbon* **40**, 1789 (2002).
- <sup>3</sup>K. C. Chin, A. Gohel, H. I. Elim, W. Chen, W. Ji, G. L. Chong, C. H. Sow, and A. T. Wee, *J. Mater. Res.* **21**, 2758 (2006).
- <sup>4</sup>J. Wang and W. J. Blau, *J. Phys. Chem. C* **112**, 2298 (2008).
- <sup>5</sup>J. Wang, Y. Chen, and W. J. Blau, *J. Mater. Chem.* **19**, 7425 (2009).
- <sup>6</sup>X. Liu, J. W. Haus, and M. S. Shahriar, *Opt. Express* **17**, 2696 (2009).
- <sup>7</sup>J. Wang, D. Früchtl, Z. Sun, J. N. Coleman, and W. J. Blau, *J. Phys. Chem. C* **114**, 6148 (2010).
- <sup>8</sup>Y. Song, G. Fang, Y. Wang, S. Liu, C. Li, L. Song, Y. Zhu, and Q. Hu, *Appl. Phys. Lett.* **74**, 332 (1999).
- <sup>9</sup>Y. Sun and J. E. Riggs, *Int. Rev. Phys. Chem.* **18**, 43 (1999).
- <sup>10</sup>S. R. Mishra, H. S. Rawat, S. C. Mehendale, K. C. Rustagi, A. K. Sood, R. Bandyopadhyay, A. Govindaraj, and C. Rao, *Chem. Phys. Lett.* **317**, 510 (2000).
- <sup>11</sup>L. Vivien, D. Riehl, E. Anglaret, and F. Hache, *IEEE J. Quantum Electron.* **36**, 680 (2000).
- <sup>12</sup>L. Vivien, D. Riehl, J. F. Delouis, J. A. Delaire, F. Hache, and E. Anglaret, *J. Opt. Soc. Am. B* **19**, 208 (2002).
- <sup>13</sup>J. Wang, Y. Chen, R. Li, H. Dong, Y. Ju, J. He, J. Fan, K. Wang, K. Liao, and L. Zhang, *J. Inorg. Organomet. Polym. Mater.* **21**, 736 (2011).
- <sup>14</sup>K. S. Novoselov, A. K. Geim, S. V. Morozov, D. Jiang, Y. Zhang, S. V. Dubonos, I. V. Grigorieva, and A. A. Firsov, *Science* **306**, 666 (2004).
- <sup>15</sup>M. D. Stoller, S. Park, Y. Zhu, J. An, and R. S. Ruoff, *Nano Lett.* **8**, 3498 (2008).
- <sup>16</sup>A. A. Balandin, S. Ghosh, W. Bao, I. Calizo, D. Teweldebrhan, F. Miao, and C. N. Lau, *Nano Lett.* **8**, 902 (2008).
- <sup>17</sup>C. E. N. E. Rao, A. E. K. Sood, K. E. S. Subrahmanyam, and A. Govindaraj, *Angew. Chem. Int. Ed.* **48**, 7752 (2009).
- <sup>18</sup>K. P. Loh, Q. Bao, P. K. Ang, and J. Yang, *J. Mater. Chem.* **20**, 2277 (2010).
- <sup>19</sup>Y. V. Bludov, M. I. Vasilevskiy, and N. M. Peres, *J. Appl. Phys.* **112**, 84320 (2012).
- <sup>20</sup>E. Hendry, P. J. Hale, J. Moger, A. K. Savchenko, and S. A. Mikhailov, *Phys. Rev. Lett.* **105**, 97401 (2010).
- <sup>21</sup>M. L. Nesterov, J. Bravo Abad, A. Y. Nikitin, F. J. García Vidal, and L. Martín Moreno, *Laser Photon. Rev.* **7**, L7 (2013).
- <sup>22</sup>Y. V. Bludov, D. A. Smirnova, Y. S. Kivshar, N. Peres, and M. I. Vasilevskiy, *Phys. Rev. B* **89**, 35406 (2014).
- <sup>23</sup>J. Wang, Y. Hernandez, M. Lotya, J. N. Coleman, and W. J. Blau, *Adv. Mater.* **21**, 2430 (2009).
- <sup>24</sup>G. Lim, Z. Chen, J. Clark, R. G. Goh, W. Ng, H. Tan, R. H. Friend, P. K. Ho, and L. Chua, *Nat. Photonics* **5**, 554 (2011).
- <sup>25</sup>M. Krishna, V. P. Kumar, N. Venkatramaiah, R. Venkatesan, and D. N. Rao, *Appl. Phys. Lett.* **98**, 81106 (2011).
- <sup>26</sup>X. Jiang, L. Polavarapu, S. T. Neo, T. Venkatesan, and Q. Xu, *J. Phys. Chem. Lett.* **3**, 785 (2012).
- <sup>27</sup>T. He, W. Wei, L. Ma, R. Chen, S. Wu, H. Zhang, Y. Yang, J. Ma, L. Huang, and G. G. Gurzadyan, *Small* **8**, 2163 (2012).
- <sup>28</sup>P. Chantharasupawong, R. Philip, N. T. Narayanan, P. M. Sudeep, A. Mathkar, P. M. Ajayan, and J. Thomas, *J. Phys. Chem. C* **116**, 25955 (2012).
- <sup>29</sup>M. Feng, H. Zhan, and Y. Chen, *Appl. Phys. Lett.* **96**, 33107 (2010).
- <sup>30</sup>J. Wang, D. Früchtl, and W. J. Blau, *Opt. Commun.* **283**, 464 (2010).